JOURNAL OF BACTERIOLOGY, May 2009, p. 2917–2925 Vol. 191, No. 9
0021-9193/09/$08.00+0 doi:10.1128/JB.01622-08

Residues of Heat-Labile Enterotoxin Involved in Bacterial Cell Surface Binding▽§

Benjamin Mudrak,[1] Daniel L. Rodriguez,[2] and Meta J. Kuehn[1,2]*

Departments of Molecular Genetics and Microbiology[1] and Biochemistry,[2] Duke University Medical Center, Durham, North Carolina 27710

Received 14 November 2008/Accepted 19 February 2009

Enterotoxigenic *Escherichia coli* (ETEC) is a leading cause of traveler's diarrhea worldwide. One major virulence factor released by this pathogen is the heat-labile enterotoxin LT, which upsets the balance of electrolytes in the intestine. After export, LT binds to lipopolysaccharide (LPS) on the bacterial surface. Although the residues responsible for LT's binding to its host receptor are known, the portion of the toxin which mediates LPS binding has not been defined previously. Here, we describe mutations in LT that impair the binding of the toxin to the external surface of *E. coli* without altering holotoxin assembly. One mutation in particular, T47A, nearly abrogates surface binding without adversely affecting expression or secretion in ETEC. Interestingly, T47A is able to bind mutant *E. coli* expressing highly truncated forms of LPS, indicating that LT binding to wild-type LPS may be due primarily to association with an outer core sugar. Consequently, we have identified a region of LT distinct from the pocket involved in eukaryotic receptor binding that is responsible for binding to the surface of *E. coli*.

Enterotoxigenic *Escherichia coli* (ETEC), a common etiologic agent behind traveler's diarrhea, is also a significant cause of mortality worldwide (38). Many strains of ETEC elaborate a virulence factor called heat-labile enterotoxin or LT (34). LT is an AB_5 toxin, consisting of a single A subunit, LTA, and a ring of five B subunits, LTB (33). LTB mediates the toxin's binding properties, and LTA ADP ribosylates host G proteins, increasing levels of cyclic AMP and causing the efflux of electrolytes and water into the intestinal lumen (27, 35). Each subunit of LT is translated separately from a bicistronic message and then transported to the periplasm, where holotoxin assembly spontaneously occurs (16). Subsequent export into the extracellular milieu is carried out by the main terminal branch of the general secretory pathway (31, 36).

LT binds eukaryotic cells via an interaction between LTB and host gangliosides, primarily the monosialoganglioside GM_1 (35). The binding site for GM_1, situated at the interface of two B subunits, has been identified by crystallography (26). GM_1 binding can be strongly impaired by a point mutation in LTB that converts Gly-33 to an aspartic acid residue (37). LT is highly homologous to cholera toxin (CT), both in sequence and structure (7, 35), contributing to ETEC's potentially cholera-like symptoms (39).

Previous work in our lab has demonstrated that LT possesses an additional binding capacity beyond its affinity for host glycolipids: the ability to associate with lipopolysaccharide (LPS) on the surface of *E. coli* (20). LPS, the major component of the outer leaflet of the gram-negative outer membrane, consists of a characteristic lipid moiety, lipid A, covalently linked to a chain of sugar residues (30). In bacteria like *E. coli*, this sugar chain can be further divided into an inner core oligosaccharide of around five sugars, an outer core of four to six additional sugars, and in some cases a series of oligosaccharide repeats known as the O antigen. Lipid A itself cannot inhibit binding of soluble LT to cells containing full-length or truncated LPS, indicating that the LT-LPS interaction involves sugar residues on the surface of *E. coli* (19). The addition of the inner core sugar 3-deoxy-D-manno-octulosonic acid (Kdo) is the minimal lipid A modification required for LT binding, although longer oligosaccharide chains are preferred, and expression of a kinase that phosphorylates Kdo abrogates binding by LT (19). Competitive binding assays and microscopy with fluorescently labeled ETEC vesicles show that binding to GM_1 and LPS can occur at the same time, revealing that the binding sites are distinct (20, 23). In contrast to LT's ability to bind to the surface of ETEC, CT (or LT, when expressed heterologously) cannot bind *Vibrio* cells, presumably because Kdo is phosphorylated in *Vibrio* spp. (5).

As a result of the LT-LPS surface interaction, over 95% of secreted LT is found associated with *E. coli* outer membrane vesicles (OMVs), rather than being secreted solubly (20). OMVs are spherical structures, 50 to 200 nm in diameter, that are derived from the outer membrane but also enclose periplasmic components (24). As such, active LT is found both on the surface of an OMV and within its lumen (21). ETEC releases a large amount of OMVs (40), and these vesicles may serve as vehicles for delivery of LT to host cells.

Recent work by Holmner et al. has uncovered a third binding substrate for LT: human blood group A antigen (17, 18). This interaction was noted previously as a novel binding characteristic of artificially constructed CT-LT hybrid molecules, but it has now been shown to occur with wild-type LT as well (17, 18). LTB binding to sugar residues in the receptor molecule occurs at a site that is separate from the GM_1-binding pocket, in the same region we proposed was involved in LPS

* Corresponding author. Mailing address: Box 3711, Duke University Medical Center, Department of Biochemistry, Durham, NC 27710. Phone: (919) 684-2545. Fax: (919) 684-8885. E-mail: mkuehn@biochem.duke.edu.

§ Supplemental material for this article may be found at http://jb.asm.org/.

▽ Published ahead of print on 6 March 2009.

TABLE 1. Strains and plasmids used in this study

Strain or plasmid	Description	Relevant characteristics	Source or reference
Strains			
jf570	H10407Δ*eltA*	ETEC strain with polar insertion in *eltA* (LT deficient)	9
MK1052	H10407Δ*eltA*/pILT	jf570 carrying inducible LT plasmid; Amp^r	This work
MK1200	H10407Δ*eltA*/pILT[T47A]	jf570 carrying inducible T47A mutant; Amp^r	This work
MK1201	H10407Δ*eltA*/pILT[Q3K]	As described for MK1200, with Q3K; Amp^r	This work
MK1203	H10407Δ*eltA*/pILT[Q3L]	As described for MK1200, with Q3L; Amp^r	This work
MK1204	H10407Δ*eltA*/pILT[Y18A]	As described for MK1200, with Y18A; Amp^r	This work
MK1206	H10407Δ*eltA*/pILT[A46D]	As described for MK1200, with A46D; Amp^r	This work
MK741	DH5α *degP*::Tn*5*/pDsbA/pILT	*E. coli* K-12, *degP* knockout, carrying a plasmid copy of *dsbA* and an inducible LT plasmid; Kan^r Cm^r Amp^r	25
MK1207	DH5α *degP*::Tn*5*/pDsbA/pILT[T47A]	As described for MK741, with inducible T47A; Kan^r Cm^r Amp^r	This work
MK1208	DH5α *degP*::Tn*5*/pDsbA/pILT[Q3K]	As described for MK1207, with Q3K; Kan^r Cm^r Amp^r	This work
MK1210	DH5α *degP*::Tn*5*/pDsbA/pILT[Q3L]	As described for MK1207, with Q3L; Kan^r Cm^r Amp^r	This work
MK1211	DH5α *degP*::Tn*5*/pDsbA/pILT[Y18A]	As described for MK1207, with Y18A; Kan^r Cm^r Amp^r	This work
MK1213	DH5α *degP*::Tn*5*/pDsbA/pILT[A46D]	As described for MK1207, with A46D; Kan^r Cm^r Amp^r	This work
CWG311	F470 *waaV*::*aacC1*	R1 core, lacks O antigen; Gm^r	15
CWG309	F470 *waaT*::*aacC1*	R1 core, two terminal Gal residues removed; Gm^r	15
CWG303	F470 *waaG*::*aacC1*	R1 core, entire outer core removed; Gm^r	15
WBB01	JC7236 Δ*waaCF*::*tet6*	Expresses only Kdo2-lipid A; Tet^r	3
Plasmids			
pILT		IPTG-inducible LT holotoxin; Amp^r	This work
pDsbA		*dsbA* ligated into pACYC184; Cm^r Tet^r	This work

binding (17, 19). While the severity of cholera disease symptoms has been linked to blood type (14), the effects of blood type on ETEC infection are less clear. However, it has been demonstrated that LT can use A antigen as a functional receptor in cultured human intestinal cells (11, 12), and one recent cohort study found an increased prevalence of ETEC-based diarrhea among children with A or AB blood type (29).

We set out to generate a mutation in LT that reduces its LPS binding without adversely affecting its expression, secretion, or toxicity. In this work, we present the discovery of point mutations in LTB that impair its interactions with the bacterial surface. Examination of these mutations reveals an LPS binding pocket which shares residues with the blood sugar pocket. Binding studies of mutants to bacteria with truncated LPS provide a better understanding of the roles that inner and outer core sugars play in toxin binding, and expression, secretion, and toxicity studies demonstrate which mutant is a particularly good candidate for future research. These binding mutants may lead to further discovery of the role that surface binding plays in the pathogenesis associated with ETEC infection.

MATERIALS AND METHODS

Strains and growth conditions. The bacterial strains and plasmids used are listed in Table 1. Strains were grown at 37°C in LB or CFA medium (1% Casamino Acids, 0.15% yeast extract, 0.005% $MgSO_4$, 0.005% $MnCl_2$) and maintained on LB plates (LB with 15 g/liter agar; ISC). Antibiotics were added at the following concentrations: 100 μg/ml ampicillin, 25 μg/ml chloramphenicol, and 30 μg/ml gentamicin. Transformations were carried out using a $CaCl_2$ protocol as described previously (20). A total of 200 μM isopropyl-1-thio-β-D-galactopyranoside (IPTG; Sigma) was used to induce expression of wild-type or mutant LT constructs. Y1 adrenal cells (ATCC number CCL-79) were maintained in Kaighn's medium supplemented with 10% fetal calf serum. Unless specified, reagents were purchased from VWR.

Construction of pILT. An IPTG-inducible LT holotoxin construct was generated by cloning the coding sequence of *eltAB* from pPLT (20). The operon's sequence was amplified by PCR using primers eltABforward and eltABreverse, which include restriction sites for BamHI and PstI, respectively (Table 2). PCR products were digested with BamHI and PstI (NEB) and then ligated into similarly digested pTrc99A vector (GE Healthcare) to form pILT.

Mutagenesis. Site-directed mutagenesis was performed on pILT using the QuikChange kit (Qiagen), according to the manufacturer's instructions. Primers used are listed in Table 2 and Table S1 in the supplemental material. All mutations were verified by sequencing at the Duke University DNA Analysis Facility. Mutants are named by combining the original amino acid residue, its position in the primary sequence of LTB after cleavage of the signal sequence, and the new substituted amino acid. In each case, the presence of only the desired mutation was confirmed by sequencing (data not shown).

Construction of pDsbA. A plasmid carrying *dsbA* was generated by amplification of the *dsbA* gene sequence from DH5α genomic DNA, using primers dsbABamHIfwd and DsbA-R(XbaI), which feature the indicated restriction sites (Table 2). PCR products were digested with BamHI and XbaI (NEB) and ligated into similarly digested pACYC184 vector to form pDsbA.

Toxin purification. Toxin was prepared from MK741 or a derivative thereof expressing mutant toxin. This strain background is DegP deficient and overexpresses DsbA in order to maximize the yield (41). Cells were diluted 1:50 in CFA medium from an overnight culture and grown to an optical density at 600 nm (OD_{600}) of ~0.8 and then induced overnight. The next morning, the periplasm

TABLE 2. Oligonucleotides used in this study

Primer	Sequence (5′→3′)[a]
ltbY18Asense	CACAACACACAAATA**GCC**ACGATAAATGACAAG
ltbY18Aantisense	CTTGTCATTTATCGT**GGC**TATTTGTGTGTTGTG
ltbQ3Lsense	CACACGGAGCTCCT**CTG**TCTATTACAGAACTATG
ltbQ3Lantisense	CATAGTTCTGTAATAGA**CAG**AGGAGCTCCGTGTG
ltbQ3Ksense	CACACGGAGCTCCT**AAA**TCTATTACAGAACTATG
ltbQ3Kantisense	CATAGTTCTGTAATAGA**TTT**AGGAGCTCCGTGTG
ltbT47Asense	GAGCGGCGCA**GCA**TTTCAGGTCGAAGTCCC
ltbT47Aantisense	GGGACTTCGACCTGAAA**TGC**TGCGCCGCTC
ltbA46Dsense	CATTACATTTAAGAGCGGC**GAC**ACATTTCAGGTCG
ltbA46Dantisense	CGACCTGAAATGT**GTC**GCCGCTCTTAAATGTAATG
eltABforward	CG*GGATCC*CGCCTCGATGAAAAATATAAC
eltABreverse	AA*CTGCAG*AACCAATGCATTGGCTAGTTTCCATAC TGATTG
dsbABamHIfwd	CG*GGATCC*CGGAAGAATTTAGCGAGTTC
DsbA-R(XbaI)	GC*TCTAGA*GCTCCCTGATAAAACAGCAA

[a] Mutagenic codons are bold; restriction sites are italic.

was harvested by osmotic shock essentially as described previously (4). One milliliter of periplasm was incubated at 4°C overnight with 100 μl of 20% immobilized D-galactose beads (Pierce) in TEN (50 mM Tris [pH 7.5], 1 mM EDTA, 200 mM NaCl). For some mutants, phenylmethylsulfonyl fluoride (Sigma) was added to a final concentration of 1 mM to prevent degradation. Beads were pelleted at 700 × *g*, washed with TEN, and then resuspended in 1 ml 0.3 M galactose in TEN. Finally, beads were pelleted at 4,000 × *g* for 5 min, and soluble toxin was retained. Purified toxin was concentrated in 10-kDa-cutoff Ultra-4 centrifugal filters (Amicon) and assayed for protein concentration using Coomassie Plus reagent (Pierce). Toxin was assessed for purity by sodium dodecyl sulfate-polyacrylamide gel electrophoresis and protein staining with Ruby Red (Molecular Probes).

Assessment of holotoxin formation. Purified wild-type and mutant toxins (400 ng) were loaded on 15% polyacrylamide gels and analyzed by immunoblotting as described previously (20, 32) with mouse monoclonal anti-LTA (Abcam) or cross-reactive rabbit polyclonal anti-CT (Sigma).

GM_1 enzyme-linked immunosorbent assay (ELISA). Purified GM_1 (1 μg/ml in phosphate-buffered saline [PBS], pH 7.2; Sigma) was added to 96-well medium-binding enzyme immunoassay/radioimmunoassay plates (Corning) and adsorbed for at least 1 h at 25°C. All other incubations were at 25°C for 1 h with volumes of 100 μl/well unless otherwise noted. After washing with PBS, 360 μl/well of buffer A (20 mM Tris [pH 7.4], 0.15 M NaCl, 0.1% bovine serum albumin [BSA], 5 mM $CaCl_2$) was added to block. After one wash with PBS, samples (diluted in buffer A) were added. Purified toxins were tested at a concentration of 1 nM (corresponding to ~10 ng toxin per well); cell-free supernatant was diluted 1:3, and periplasm was diluted 1:20. Following three washes, the plate was incubated with rabbit anti-CT primary antibody (Sigma) at a 1:10,000 dilution in PBS. The plate was then washed three times with PBST (PBS with 0.05% Tween 20) and incubated with secondary antibody (1:10,000) (anti-rabbit immunoglobulin G conjugated to horseradish peroxidase; Sigma). After three final PBST washes, OptEIA substrate (BD) was added for 5 min. Stop solution (2 N H_2SO_4) was added, and the A_{410} was measured using a FluoSTAR Optima microplate reader (BMG Labtech). Background absorbance from blank wells was subtracted from all other values.

Toxicity assay. A bioassay on Y1 cells was performed in duplicate as described previously (21).

Blood trisaccharide ELISA. Blood group A terminal trisaccharide (GalNAcα3[Fucα2]Gal) conjugated to BSA (5 μg/ml in 0.1 M $NaHCO_3$; vLabs) was adsorbed to 96-well PolySorp plates (Nunc) at 25°C for at least 1 h. All other incubations were at 25°C for 1 h with volumes of 100 μl/well unless otherwise noted. After three washes with wash buffer, 360 μl/well of blocking/binding buffer was added. Wells were washed three times, and samples were added. All samples consisted of purified toxin at a final concentration of 1 nM in binding buffer (~10 ng toxin per well). The remaining steps were the same as used for the GM_1 ELISA, but wash buffer was used for all washes and antibodies were diluted in binding buffer. Blocking/binding buffer and wash buffer were made as previously described (6).

Cell surface binding assay. Two milliliters of cells in mid-log phase (OD_{600}, ~0.5 to 0.7) were pelleted and resuspended in ice-cold HEPES (50 mM, pH 6.8). Purified toxin was added to a final concentration of 500 nM (to jf570 cells) or 100 nM (all other strains) with TEN buffer added for a final volume of 0.2 ml, and the mixture was incubated with shaking at 4°C for 1 h. Cells were pelleted, and supernatants containing unbound toxins were collected. Cell pellets were washed once and then resuspended in 0.2 ml HEPES. Resuspended cells were concentrated by precipitation with 20% trichloroacetic acid (TCA). Fractions containing unbound toxin were also concentrated with TCA after the addition of 100 μg of BSA as a carrier. Equal volumes of precipitate resuspended in sample buffer were loaded on a 15% polyacrylamide gel and analyzed by immunoblotting with cross-reactive anti-CT as described previously (20). The amount of toxin associated with the cells in each sample was quantified by densitometry of the LTB bands in the linear range of the immunoblot using ImageJ software (NIH). Each assay was performed using a separate batch of purified toxin. For competition assays, toxin was preincubated for 1 h at 25°C with buffer, BSA, or blood group A trisaccharide conjugated to BSA at a 20-fold molar excess before being added to DH5α cells as described above. For some experiments, pronase (Sigma) was added to resuspended WBB01 cells at a final concentration of 0.1 mg/ml and the mixture was incubated for 15 min at 37°C as previously described (20). Cells were then washed three times with HEPES before the addition of toxin as described above.

Fluorescence-based cell surface binding assay. DH5α cells were incubated with buffer, wild-type LT, and T47A and then washed and resuspended identically to the binding assay described above. Then, 100 μl of 1 μM BODIPY-GM_1 (Molecular Probes) diluted in methanol was added to each sample, and the mixtures were incubated for 30 min at 4°C. Following three washes with 50 mM HEPES plus 0.1% Triton X-100 (pH 6.8), pellets were resuspended in 210 μl of HEPES and 100 μl was applied to each of two wells in a black polystyrene 96-well plate (Corning). Fluorescence was measured using a FluoSTAR Optima (excitation, 485 nm; emission, 520 nm). Values for cells incubated with buffer alone were subtracted from the other samples as background fluorescence and nonspecific binding.

Cell fractionation. Strains were diluted 1:50 from overnight cultures, grown for 2 to 4 h at 37°C to an OD_{600} of ~0.8, and induced overnight. The next morning, a sample of total culture was precipitated with 20% TCA. Each strain was serially plated for CFU, and the remaining cells were pelleted at 6,000 × *g* for 10 min. CFU-matched samples were compared by immunoblotting with anti-CT. The supernatant was collected, and the periplasm was isolated essentially as described previously (21). Both supernatant and periplasmic fractions were passed through a 0.45-μm syringe filter (Pall). Periplasmic alkaline phosphatase activity was measured using the SensoLyte kit (AnaSpec) according to the manufacturer's instructions.

Statistical analysis. Results were analyzed by analysis of variance; values of $P < 0.05$ were considered statistically significant.

RESULTS

Mutagenesis and assessment of proper assembly of mutant toxins. Given the recent identification of a peripheral sugar binding pocket on LTB by cocrystallization (17), we investigated whether or not this region also plays a role in LPS binding. Residues Gln-3, Tyr-18, Ala-46, and Thr-47 were shown to interact directly with blood sugar antigen (17). Mutations were designed to introduce a highly dissimilar amino acid residue in place of the native residue, and the residues were mutagenized in a plasmid containing an inducible LT construct (pILT), generating the following mutants: Q3K, Q3L, Y18A, A46D, and T47A.

In order to verify that each was folded and assembled, mutant toxins were subjected to multiple assays to assess holotoxin formation following purification. First, wild-type and mutant toxins were immunoblotted using an anti-LTA monoclonal antibody. All toxins were detected equally (Fig. 1A). The purification process is based on galactose binding by LTB pentamers, so detection of equal amounts of LTA in purified samples is a positive indication of holotoxin assembly. Levels of purified LTB were also equal as compared by Ruby Red staining of sodium dodecyl sulfate-polyacrylamide gels or immunoblotting with cross-reactive anti-CT antibody (Fig. 1A and data not shown).

This same panel of purified toxins was also tested for the ability to bind the eukaryotic receptor GM_1 by ELISA. Since GM_1 binding involves residues in adjacent B subunits, this assay serves as an indication of wild-type folding and pentamer assembly. The Q3K, Q3L, and Y18A mutants bound GM_1 at wild-type levels, while the T47A mutant did show a slight, but statistically significant, reduction in binding to approximately 89% of that of the wild type ($n = 4$) (Fig. 1B). The A46D mutant demonstrated a stronger impairment of GM_1 binding to approximately 55% of that of the wild type ($n = 3$) (Fig. 1B).

Lastly, each mutant was tested for toxicity using a previously described in vitro cell culture bioassay based on a morphological change in Y1 adrenal cells (8). Each mutant exhibited toxic effects comparable to wild-type LT (4 to 8 ng of each elicited maximal rounding of 4×10^5 cells). Taken together, our results indicate that these mutations do not appreciably alter the proper folding of LT, although the A46D mutant does somewhat impair host receptor binding.

Mutations in LT's blood sugar binding pocket also impair bacterial surface binding. In order to biochemically validate the role of Gln-3, Tyr-18, Ala-46, and Thr-47 in blood sugar binding,

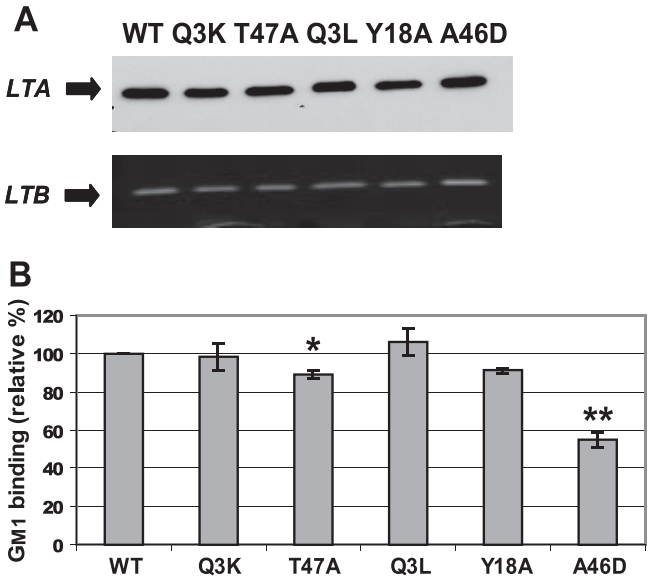

FIG. 1. Mutant LT B subunits assemble into holotoxins that bind GM_1. (A) Representative immunoblot (top) and Ruby Red protein stain (bottom) of 400 ng each of purified wild-type toxin (WT) or the indicated mutant toxins. The blot was probed with anti-LTA antibody. (B) Relative GM_1 binding of purified toxins, as measured in quadruplicate by ELISA. Wild-type toxin binding was set to 100%. *, $P < 0.05$; **, $P < 0.005$ compared to that of the wild type ($n \geq 2$).

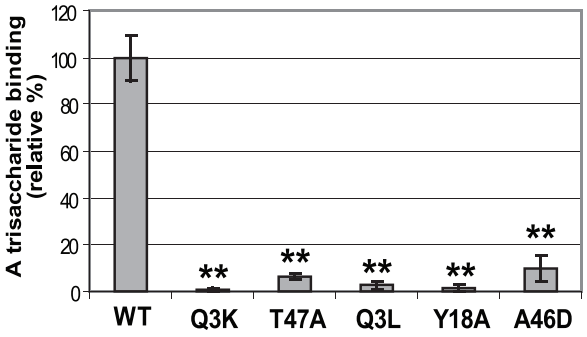

FIG. 2. Alteration of putative sugar binding residues in LTB abolishes toxin binding to blood antigen sugars. Relative binding of wild-type toxin (WT) and the indicated mutant toxins to blood group A antigen trisaccharide conjugated to BSA. Wild-type toxin binding was set to 100%. Each ELISA was carried out in quadruplicate, and at least two different batches of purified toxin were tested. **, $P < 0.005$ compared to that of the wild type ($n \geq 3$).

toxins containing the respective point mutations were tested for the ability to bind blood group A trisaccharide. Each mutation drastically impaired the toxin's ability to bind A trisaccharide in an ELISA-based assay (Fig. 2). For Q3K, Q3L, and Y18A mutants, the level of absorbance detected in some trials was equivalent to that of the blank, indicating a complete loss of binding. We have therefore demonstrated that four residues identified by cocrystallography (Gln-3, Tyr-18, Ala-46, and Thr-47) are indeed required for LT to associate with blood sugars.

To examine whether any of these blood sugar binding mutants were impaired in LPS binding, purified mutant toxins were screened using a bacterial cell surface binding assay. After incubation and washing, we assessed the level of each toxin associated with *E. coli* by immunoblotting (Fig. 3A). Initial screening of the cell surface binding was carried out using DH5α cells due to the defined oligosaccharide core structure and consistent length of its LPS (Fig. 3B) and because previous work from our laboratory demonstrated no essential involvement of O antigen in the LT-LPS interaction (19). Densitometric analysis of multiple immunoblots revealed that mutants Q3K, T47A, Q3L, and A46D possess a clearly reduced capacity to bind bacterial cells in vitro (Fig. 3C). Of these, the T47A and A46D mutants showed the strongest impairment, with the T47A mutant nearly abolishing surface binding. Mutant Y18A bound the cell surface at wild-type levels, in contrast to its lack of binding to blood group A trisaccharide. In each case, unbound toxin was detectable in the supernatant after pelleting the cells, indicating that the toxin was not degraded during the assay (Fig. 3D).

Surface binding of exogenously added wild-type LT and T47A mutant was also compared using fluorescently labeled GM_1 to detect bound toxin. The T47A mutant was detected at a significantly reduced level after subtraction of fluorescence from nonspecific binding (42.2% ± 7.5% of that of the wild type; $n = 4$; $P < 0.0005$). Measurements using fluorescent GM_1 did not show as strong an impairment for the T47A mutant, as our immunoblot-based assay could not distinguish intermediate levels of impairment (e.g., that of Q3K), since fluorescent GM_1 had a relatively high background of nonspecific binding (with a value near T47A's before correction) and a tendency to aggregate. Nevertheless, this independent assay supports our assertion that T47A's binding to the bacterial surface is impaired.

Since similar residues appeared to be responsible for binding to both blood sugars and the bacterial surface, we expected that blood sugars could inhibit bacterial surface binding. Consistent with this hypothesis, preincubation of LT with an excess of A trisaccharide conjugated to BSA, but not BSA alone, abolished subsequent binding to the bacterial surface (Fig. 4). In contrast, preincubation of LT with A trisaccharide conjugated to BSA or BSA alone had no significant effect on GM_1 binding (data not shown). Therefore, the blood sugar and bacterial surface binding sites of LT overlap but are not identical, and both sites are distinct from the GM_1 binding pocket.

It should be noted that we generated mutations in 10 other residues on the periphery of LTB, including many in areas that we had previously speculated may play a role in LPS binding (19). However, these additional mutants exhibited either poor expression in ETEC or had no effect on surface binding in preliminary experiments and were therefore set aside (Table 3).

Binding of T47A and A46D mutants to bacteria expressing truncated forms of LPS. Previous work from our lab has shown that LT requires only the innermost LPS core sugar, Kdo, for binding, although it binds better to LPS with a full oligosaccharide core (19). To determine whether the T47A and A46D mutations affected binding to Kdo or other core sugars, we repeated our cell surface binding assay with strains containing truncated forms of LPS from an F470 background. CWG311 features an R1 LPS core, which is similar to the K-12 *E. coli* core found in DH5α, and a disruption in *waaV* to prevent ligation of O antigen (15). CWG309 and CWG303 feature

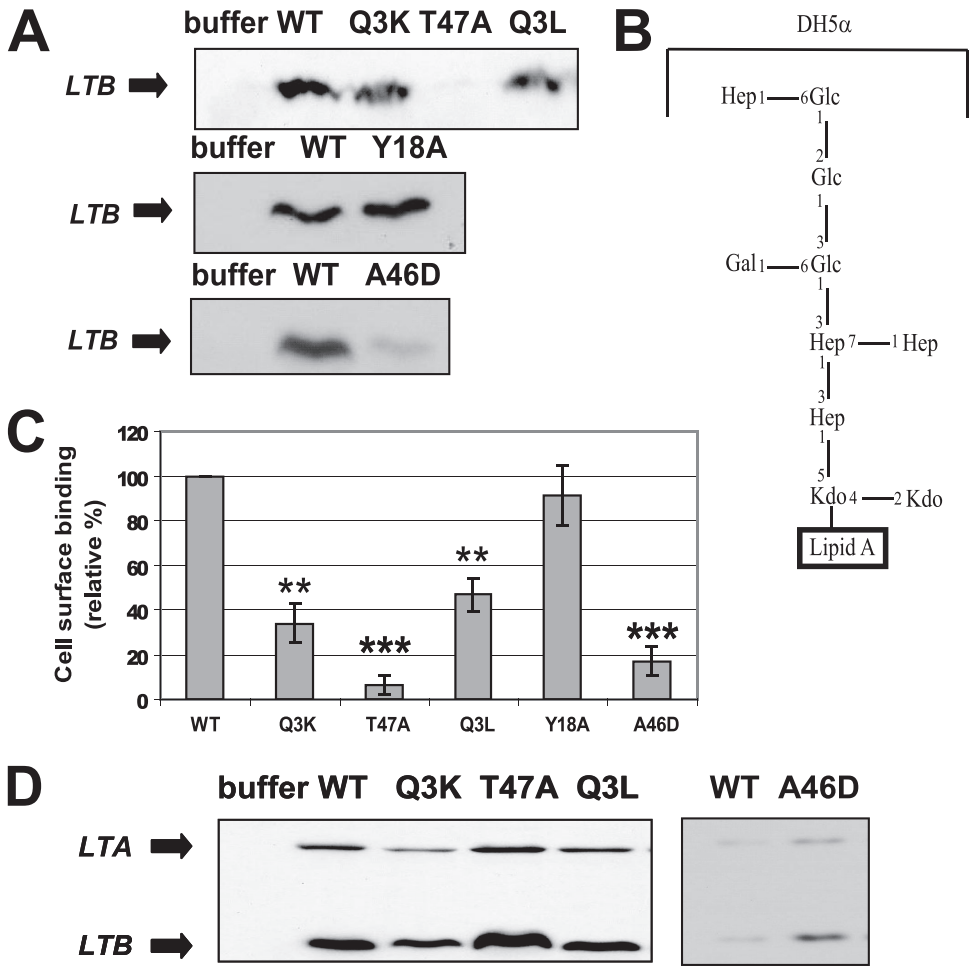

FIG. 3. Mutations in LT's blood antigen binding pocket impair association of the toxin with the *E. coli* cell surfaces. (A) Representative immunoblots of DH5α cells after incubation with buffer, wild-type toxin (WT), or the indicated mutant toxin. (B) Structure of the K-12 oligosaccharide core carried by DH5α (adapted from reference 10). (C) Shown are relative binding levels of the wild-type toxin and indicated mutant toxins to DH5α cells. Binding of the wild-type toxin was set to 100%. Each experiment was carried out using a fresh batch of purified toxin. **, $P < 0.005$; ***, $P < 0.0005$ ($n = 3$). (D) Immunoblots of unbound toxin in the supernatant fraction from the incubations described for panel A. Blots were probed with cross-reactive anti-CT antibody.

other mutations in this background, truncating LPS to various extents (Fig. 5A). Specifically, CWG309 (Δ*waaT*) lacks two terminal galactose residues from the R1 core, and CWG303 (Δ*waaG*) lacks two additional residues, both glucoses, leaving only three heptose residues and two Kdo residues (10, 15). WBB01 is derived from a different strain background and carries deletions in both heptosyltransferases of *E. coli* (3), preventing the addition of sugars beyond the two innermost Kdo residues. As a result, WBB01 expresses Kdo2-lipid A, the minimal viable LPS structure in *E. coli* and the portion conserved across all *E. coli* oligosaccharide core types (2, 30). Since changes in LPS structure affect outer membrane protein and lipid composition (28), comparisons between WT and mutant toxin binding could be made for each strain but not between strains.

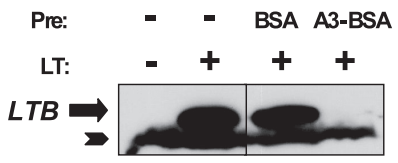

FIG. 4. Blood group A trisaccharide inhibits binding of LT to the surface of *E. coli*. Representative immunoblot of LT bound to DH5α cells ($n = 3$). Toxin was preincubated (Pre) with buffer (−), BSA, or blood group A trisaccharide conjugated to BSA (A3-BSA). Blots were probed with cross-reactive anti-CT antibody. Arrowhead indicates nonspecific band detected.

The T47A mutant showed a strong impairment in binding to the full R1 oligosaccharide core and the same core lacking its two terminal galactose sugars (Fig. 5B and C). However, the mutation does not seem to affect binding to CWG303 at all or binding to WBB01 to any large extent (Fig. 5D and E). Pretreatment of WBB01 cells with pronase did not affect the levels of bound T47A (data not shown). Therefore, the T47A mutant retains the ability to bind Kdo but is impaired for binding to fuller core structures. In contrast, the A46D mutant demon-

TABLE 3. Expression levels of LTB mutants in ETEC

Mutation	Codon change[a]	Blood sugar binding pocket location[f]	Expression level in ETEC[b]
Q3K	CAG→AAA	In	Wild type
Q3L	CAG→CTG	In	Poor
Y18A	TAT→GCC	In	Poor
K23A	AAG→GCG	Out	Only LTA detected
L25E	CTA→GAA	Out	Wild type
L25I	CTA→ATC	Out	Poor
F42E	TTT→GAG	Out	None detected
F42Y	TTT→TAT	Out	None detected
K43R	AAG→CGT	Out	Wild type[c]
A46D	GCA→GAC	In	Reduced
A46S	GCA→AGC	In	Reduced
T47A	ACA→GCA	In	Wild type
F48Y	TTT→TAT	Out	None detected
Q49L	CAG→CTG	Out	Wild type[c]
T80A[d]	ACC→GCC	Out	Wild type[c]
D83L	GAT→CTG	Out	Poor
N94L[e]	AAT→CTG	In	Wild type[c]
S100K	AGT→AAA	Out	Poor
S100L	AGT→CTG	Out	Poor

[a] Oligonucleotides used to generate these mutants are listed in Table 2 (see Table S1 in the supplemental material).
[b] LTB mutants were transformed into jf570, and expression level was examined by immunoblot analysis of CFU-matched total culture samples using cross-reactive anti-CT antibody.
[c] Mutant also exhibited wild-type behavior in preliminary cell surface binding assays.
[d] This mutant was generated using XL-1 Red mutator cells (Stratagene), according to the manufacturer's instructions; it also has a silent mutation at Tyr-15 (ACA→ACT).
[e] This residue's interaction with blood sugar residues is only through its backbone.
[f] In, inside; Out, outside.

strates a similar binding deficiency to all strains tested (Fig. 5B to D).

Surface binding of the T47A mutant in ETEC. Since the T47A mutant was a fully folded mutant toxin deficient in binding to wild-type strains of *E. coli*, further studies were focused on this mutation. The surface features of ETEC and laboratory *E. coli* strains differ in many ways, so we next tested a more biologically relevant scenario: the binding of the T47A mutant to the surface of ETEC. An LT-deficient ETEC strain, H10407Δ*eltA* (jf570), was used. This strain contains a polar insertion in *eltA*, the first gene in the operon encoding LT, thus abolishing production of the toxin (9). The T47A mutant exhibited a nearly complete lack of binding to jf570 cells using our surface binding assay (Fig. 6A and B). Once again, the lack of binding was not due to degradation, since the T47A mutant was detected in the unbound fraction (Fig. 6C).

Characterization of T47A expression and secretion in ETEC. In order to assess the behavior of the T47A mutant when expressed in vivo, an inducible LT plasmid with the T47A mutation introduced was transformed into jf570. After induction overnight, toxin expression levels were determined by immunoblotting total culture samples which had been concentrated by TCA precipitation. The levels of the T47A mutant matched those of the wild type (Fig. 7A).

To examine whether the T47A mutation affected secretion of LT by ETEC, cultures of strains carrying wild-type LT and T47A were induced and fractionated. Levels of toxin in the supernatant were measured by GM_1-binding ELISA, with data normalized to CFU. The T47A mutant was found in the supernatant at levels slightly higher than that of the wild type (Fig. 7B). A corresponding decrease in the levels of the T47A mutant in the periplasm was noted as well (Fig. 7B). Thus, the numerous properties of LT, including expression, holotoxin assembly, secretion, and host receptor binding, are not significantly affected by the T47A mutation, only the toxin's ability to bind the bacterial surface.

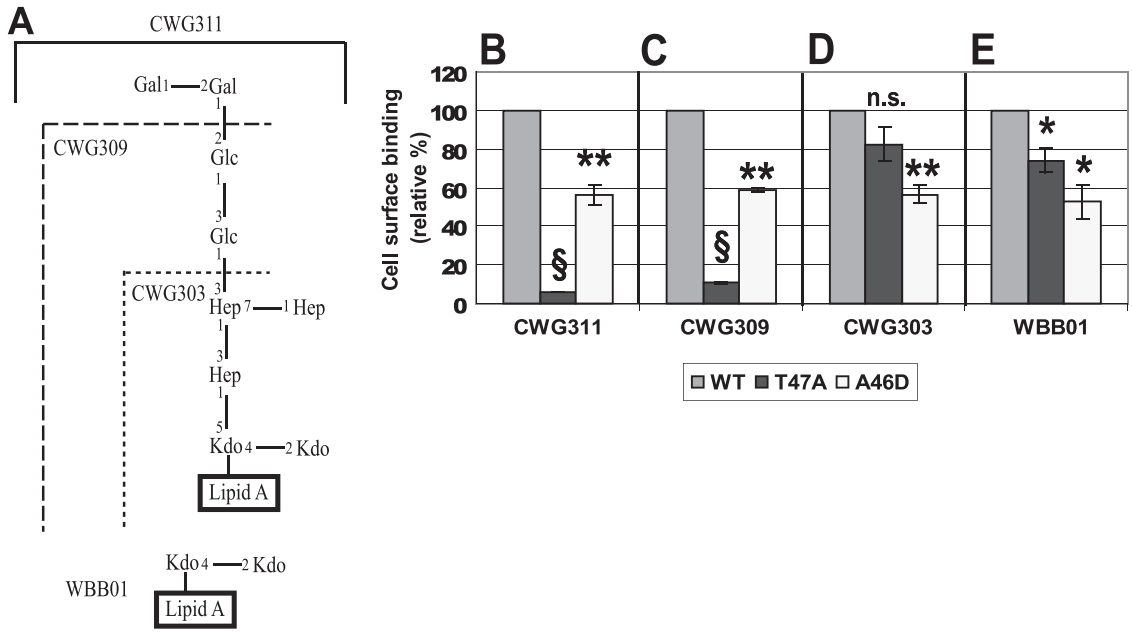

FIG. 5. The T47A and A46D mutants bind the surface of *E. coli* expressing truncated LPS. (A) Structure of the R1 LPS oligosaccharide core carried by CWG311, with truncations present in strains CWG309 and CWG303 indicated (adapted from reference 10). The LPS structure of WBB01 is also depicted. Shown are relative binding of wild-type toxin (WT) and the indicated mutant toxins to CWG311 (B), CWG309 (C), CWG303 (D), and WBB01 (E). Binding of WT toxin was set to 100% for each strain. Each experiment was carried out using a fresh batch of purified toxin. *, $P < 0.05$; **, $P < 0.001$; §, $P < 0.0001$; n.s. = not significant compared to wild type ($n \geq 2$).

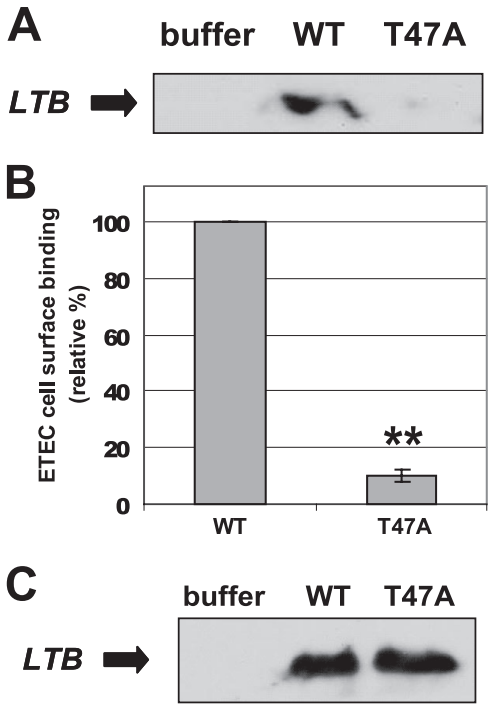

FIG. 6. The T47A mutant does not bind the surface of ETEC. (A) Representative immunoblot of jf570 ETEC cells after incubation with buffer, wild-type toxin (WT), or T47A mutant toxin. (B) Relative binding of the wild-type and T47A toxins to ETEC cells are shown. Binding of the wild-type toxin was set to 100%. Each experiment was carried out using a fresh batch of purified toxin. **, $P < 0.001$ ($n = 2$). (C) Immunoblot of unbound toxin from supernatant of incubations as described for panel A. Blots were probed with cross-reactive anti-CT antibody.

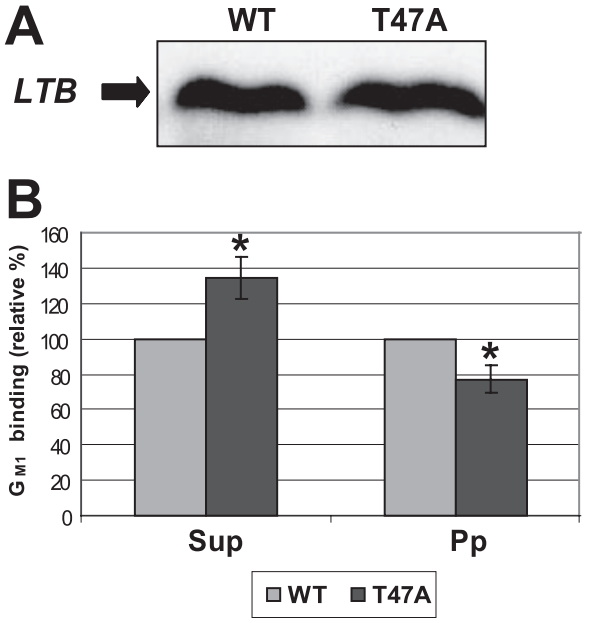

FIG. 7. The T47A mutant is expressed at wild-type levels but demonstrates altered localization in ETEC culture fractions. (A) Representative immunoblot of TCA-precipitated total culture samples, adjusted for CFU, demonstrating induced expression levels of the wild type (WT) and T47A mutant in ETEC. The blot was probed with cross-reactive anti-CT antibody. (B) MK1052 (wild type) and MK1200 (T47A) were fractionated to isolate cell-free supernatant (Sup) and periplasm (Pp). Each fraction was tested for toxin levels by GM_1 ELISA. Supernatant levels were normalized to CFU, and periplasm levels were normalized to alkaline phosphatase activity. *, $P < 0.05$ ($n = 4$).

DISCUSSION

Previous work in our lab defined an interaction between LT produced by ETEC and the sugar moieties in LPS on the bacterial surface that was not dependent on the GM_1 binding site (19). A recent report revealed a second sugar binding pocket at the interface of two B subunits on the periphery of LT (17), leading us to investigate whether that region may also be responsible for binding to LPS. Mutation of this binding pocket confirmed that the area defined by Ala-46, Thr-47, and Gln-3 of adjacent B subunits is necessary for binding to blood group A antigen and is also critical for binding the bacterial cell surface. Both blood antigens and LPS contain complex polysaccharides. With five binding sites per holotoxin, one at each interface between adjacent B subunits, LT may interact with one or more LPS molecules at various places along the sugar chain. With that in mind, it is notable that the mutation of multiple residues was not required in order to disrupt blood group sugar or LPS binding. Similarly, a single amino acid substitution is sufficient to disrupt oligomerization of B subunits (22) and to abolish binding to the eukaryotic receptor GM_1 (37). Thus, single point mutations can impair each of LT's binding properties, highlighting the exquisitely fine-tuned relationship between structure and function in the toxin.

Our analysis of the T47A mutation supports our previous observation that LT's association with LPS is based on binding to multiple core sugar residues in LPS, although binding to Kdo2-lipid A is possible. The T47A mutant is unable to bind *E. coli* cells featuring a full core but is able to bind to Kdo when made available by truncation of surface LPS molecules (Fig. 5). Additionally, while much less T47A mutant associated with liposomes composed of purified full-length LPS than wild-type LT, both toxins bound at a similarly low level to Kdo2-lipid A liposomes (D. L. Rodriguez and M. J. Kuehn, unpublished observations). Therefore, it appears that the primary binding target of wild-type LT, one that is critically dependent on Thr-47, is a sugar residue other than Kdo. Only for truncated LPS does the alternative substrate Kdo become a significant factor, presumably due to the contribution of other residues in the area or possibly to a separate binding pocket altogether. These results are in line with our previous observations that wild-type LT is competed off the surfaces of cells expressing Kdo2-lipid A by incubation with full-length LPS, but not vice versa (19).

Perturbations to the composition of the outer membrane caused by extensive truncation of LPS in deep rough strains like CWG303 and WBB01 (28) make comparisons of LT binding across the LPS truncation strain panel difficult. Additionally, some membrane instability has been reported previously for CWG303, in particular (42). Thus, comparisons of LT binding to full-length and truncated LPS would best be made with an assay based on purified LPS, and such efforts are underway.

In contrast to the binding profile of the T47A mutant, the A46D mutant showed a significant, consistent deficiency in cell surface association, regardless of the length of LPS (Fig. 5). This result is most likely due to the nature of the amino acid substitution. Introduction of a large, charged aspartate residue in place of the small nonpolar alanine may have resulted in an overall destabilization of the binding pocket. As such, the mutant can bind to the same substrates as wild-type LT, but with a lower affinity in general. In fact, the impact of this mutation may extend beyond the local region, as A46D also demonstrated a similar decrease in GM_1 binding. Since the binding pockets for the cell surface and GM_1 are both at the interface of two adjacent subunits, it is possible that the introduction of a bulky aspartate residue alters the spacing of the pentameric LTB ring, thus impairing all binding properties of the toxin. Interestingly, there was a noticeable difference between the levels of A46D binding to two strains featuring full LPS cores, DH5α and CWG311 (Fig. 3C and 5B). This disparity may be the result of the slight differences in core residue linkages found between the two strains, with A46D less able to accommodate binding to DH5α's K-12 core.

Our data demonstrate overlapping yet distinct LT-LPS and LT-blood sugar binding interfaces, characterized by differences in binding properties of the Gln-3 and Tyr-18 mutants. Whereas the T47A mutation strongly impaired binding to both blood sugars and bacteria with full LPS cores, the Q3K mutation totally abolished blood sugar binding but only reduced surface binding by 66% (Fig. 2 and 3C). It is likely that the residues in the binding pocket vary in their contributions to each intermolecular interaction and that each substrate can accommodate different alterations to the residues in the binding pocket. This point is further supported by the Y18A mutation. While Tyr-18 plays a critical role in blood sugar binding, it is dispensable for binding the bacterial surface (Fig. 2 and 3C). Furthermore, like Y18A, CT does not contain a tyrosine residue at that position yet is still able to bind the surface of *E. coli* (19).

The toxin harboring a T47A mutation was the focus of further studies in ETEC since this mutation does not appear to adversely affect any properties of the toxin besides binding to the surface of *E. coli* and blood group antigen (Fig. 1 to 3). There was a small reduction in GM_1 binding capacity, but this result may reflect a small contribution by the blood sugar pocket to GM_1 binding. This speculation is based on the fact that blood group A antigen and GM_1 each feature a galactose residue which is involved significantly in binding to LT (17, 26) and that G33D, the GM_1-binding mutant of LTB, retains some ability to bind immobilized galactose (13). Thus, for T47A, the reduced ability of the peripheral pocket to bind galactose may also slightly reduce binding to GM_1.

Our assessment of surface binding to ETEC reveals that the impairment detected for T47A is not limited to laboratory strains (Fig. 6). Further characterization of T47A's behavior in vivo revealed comparable expression of wild-type LT and T47A in ETEC. Unlike T47A, most of the blood sugar binding mutants described above and many other LTB point mutants we generated displayed poor stability when expressed in ETEC (Table 3). Presumably, even small changes in the primary structure of LTB render it more susceptible to degradation by proteases expressed by ETEC. In some cases, the yield of these mutants was considerably reduced when they were expressed in a DegP-deficient DH5α strain, indicating an inherent instability.

We examined secreted and cellular ratios of toxin and noted slightly increased levels of secreted T47A and slightly decreased levels of periplasmic T47A (Fig. 7). The difference between levels of wild-type LT and T47A detected during fractionation ultimately may be due to T47A's deficiency in cell surface binding. That is, when cells expressing equivalent amounts of wild-type and T47A toxin are initially pelleted from culture, they will pull down less T47A than the wild type. As a result, the level of T47A toxin remaining in the cell-free supernatant will be relatively higher. It is also likely that material bound to the cell surface is released during periplasm preparation so that cells expressing T47A, which binds poorly to the bacterial surface, would release less toxin into the soluble periplasm fraction than cells expressing wild-type LT. Thus, the behavior of toxins expressed in ETEC reinforces the surface binding data based on exogenously added toxin. However, our data do not rule out the possibility that T47A is secreted more efficiently than wild-type LT.

LT is able to mediate the internalization of intact OMVs into host cells (23), and expression of the toxin provides an advantage during the initial colonization of the small intestine (1). The T47A mutation generates a bacterial surface binding LT mutant that is free from defects in expression, assembly, secretion, and holotoxin activity. T47A creates a CT-like scenario in which secreted LT is not membrane bound, allowing for future research to address the role of the LT-LPS interaction in ETEC pathogenesis. The mutations described above also highlight the portion of the LTB molecule responsible for this interaction: a peripheral sugar binding pocket distinct from, but overlapping with, the toxin's blood sugar binding site.

ACKNOWLEDGMENTS

We thank J. Fleckenstein for generously providing H10407Δ*eltA*, C. Whitfield for strains CWG311, CWG309, and CWG303, and W. Brabetz for strain WBB01.

This work was supported by RO1A164464 and R21AI063239 from the NIAID and a Burroughs Wellcome Investigator in Pathogenesis of Infectious Disease Award (to M.J.K.).

REFERENCES

1. **Allen, K. P., M. M. Randolph, and J. M. Fleckenstein.** 2006. Importance of heat-labile enterotoxin in colonization of the adult mouse small intestine by human enterotoxigenic *Escherichia coli* strains. Infect. Immun. **74:**869–875.
2. **Amor, K., D. E. Heinrichs, E. Frirdich, K. Ziebell, R. P. Johnson, and C. Whitfield.** 2000. Distribution of core oligosaccharide types in lipopolysaccharides from *Escherichia coli*. Infect. Immun. **68:**1116–1124.
3. **Brabetz, W., S. Muller-Loennies, and H. Brade.** 2000. 3-Deoxy-D-manno-oct-2-ulosonic acid (Kdo) transferase (WaaA) and *kdo* kinase (KdkA) of *Haemophilus influenzae* are both required to complement a *waaA* knockout mutation of *Escherichia coli*. J. Biol. Chem. **275:**34954–34962.
4. **Copeland, B. R., R. J. Richter, and C. E. Furlong.** 1982. Renaturation and identification of periplasmic proteins in two-dimensional gels of *Escherichia coli*. J. Biol. Chem. **257:**15065–15071.
5. **Cox, A. D., J. R. Brisson, V. Varma, and M. B. Perry.** 1996. Structural analysis of the lipopolysaccharide from *Vibrio cholerae* O139. Carbohydr. Res. **290:**43–58.
6. **Crouch, E., Y. Tu, D. Briner, B. McDonald, K. Smith, U. Holmskov, and K. Hartshorn.** 2005. Ligand specificity of human surfactant protein D: expression of a mutant trimeric collectin that shows enhanced interactions with influenza A virus. J. Biol. Chem. **280:**17046–17056.
7. **Dallas, W. S., and S. Falkow.** 1980. Amino acid sequence homology between cholera toxin and *Escherichia coli* heat-labile toxin. Nature **288:**499–501.
8. **Donta, S. T., H. W. Moon, and S. C. Whipp.** 1974. Detection of heat-labile *Escherichia coli* enterotoxin with the use of adrenal cells in tissue culture. Science **183:**334–336.
9. **Dorsey, F. C., J. F. Fischer, and J. M. Fleckenstein.** 2006. Directed delivery

of heat-labile enterotoxin by enterotoxigenic *Escherichia coli*. Cell. Microbiol. **8:**1516–1527.
10. **Firdich, E., B. Lindner, O. Holst, and C. Whitfield.** 2003. Overexpression of the *waaZ* gene leads to modification of the structure of the inner core region of *Escherichia coli* lipopolysaccharide, truncation of the outer core, and reduction of the amount of O polysaccharide on the cell surface. J. Bacteriol. **185:**1659–1671.
11. **Galván, E. M., C. D. Diema, G. A. Roth, and C. G. Monferran.** 2004. Ability of blood group A-active glycosphingolipids to act as *Escherichia coli* heat-labile enterotoxin receptors in HT-29 cells. J. Infect. Dis. **189:**1556–1564.
12. **Galván, E. M., G. A. Roth, and C. G. Monferran.** 2006. Functional interaction of *Escherichia coli* heat-labile enterotoxin with blood group A-active glycoconjugates from differentiated HT29 cells. FEBS J. **273:**3444–3453.
13. **Guidry, J. J., L. Cardenas, E. Cheng, and J. D. Clements.** 1997. Role of receptor binding in toxicity, immunogenicity, and adjuvanticity of *Escherichia coli* heat-labile enterotoxin. Infect. Immun. **65:**4943–4950.
14. **Harris, J. B., A. I. Khan, R. C. LaRocque, D. J. Dorer, F. Chowdhury, A. S. Faruque, D. A. Sack, E. T. Ryan, F. Qadri, and S. B. Calderwood.** 2005. Blood group, immunity, and risk of infection with *Vibrio cholerae* in an area of endemicity. Infect. Immun. **73:**7422–7427.
15. **Heinrichs, D. E., J. A. Yethon, P. A. Amor, and C. Whitfield.** 1998. The assembly system for the outer core portion of R1- and R4-type lipopolysaccharides of *Escherichia coli*. The R1 core-specific beta-glucosyltransferase provides a novel attachment site for O-polysaccharides. J. Biol. Chem. **273:** 29497–29505.
16. **Hofstra, H., and B. Witholt.** 1985. Heat-labile enterotoxin in *Escherichia coli*. Kinetics of association of subunits into periplasmic holotoxin. J. Biol. Chem. **260:**16037–16044.
17. **Holmner, A., G. Askarieh, M. Okvist, and U. Krengel.** 2007. Blood group antigen recognition by *Escherichia coli* heat-labile enterotoxin. J. Mol. Biol. **371:**754–764.
18. **Holmner, A., M. Lebens, S. Teneberg, J. Angstrom, M. Okvist, and U. Krengel.** 2004. Novel binding site identified in a hybrid between cholera toxin and heat-labile enterotoxin: 1.9 Å crystal structure reveals the details. Structure **12:**1655–1667.
19. **Horstman, A. L., S. J. Bauman, and M. J. Kuehn.** 2004. Lipopolysaccharide 3-deoxy-D-manno-octulosonic acid (Kdo) core determines bacterial association of secreted toxins. J. Biol. Chem. **279:**8070–8075.
20. **Horstman, A. L., and M. J. Kuehn.** 2002. Bacterial surface association of heat-labile enterotoxin through lipopolysaccharide after secretion via the general secretory pathway. J. Biol. Chem. **277:**32538–32545.
21. **Horstman, A. L., and M. J. Kuehn.** 2000. Enterotoxigenic *Escherichia coli* secretes active heat-labile enterotoxin via outer membrane vesicles. J. Biol. Chem. **275:**12489–12496.
22. **Iida, T., T. Tsuji, T. Honda, T. Miwatani, S. Wakabayashi, K. Wada, and H. Matsubara.** 1989. A single amino acid substitution in B subunit of *Escherichia coli* enterotoxin affects its oligomer formation. J. Biol. Chem. **264:** 14065–14070.
23. **Kesty, N. C., K. M. Mason, M. Reedy, S. E. Miller, and M. J. Kuehn.** 2004. Enterotoxigenic *Escherichia coli* vesicles target toxin delivery into mammalian cells. EMBO J. **23:**4538–4549.
24. **Kuehn, M. J., and N. C. Kesty.** 2005. Bacterial outer membrane vesicles and the host-pathogen interaction. Genes Dev. **19:**2645–2655.
25. **McBroom, A. J., A. P. Johnson, S. Vemulapalli, and M. J. Kuehn.** 2006. Outer membrane vesicle production by *Escherichia coli* is independent of membrane instability. J. Bacteriol. **188:**5385–5392.
26. **Merritt, E. A., T. K. Sixma, K. H. Kalk, B. A. van Zanten, and W. G. Hol.** 1994. Galactose-binding site in *Escherichia coli* heat-labile enterotoxin (LT) and cholera toxin (CT). Mol. Microbiol. **13:**745–753.
27. **Moss, J., and S. H. Richardson.** 1978. Activation of adenylate cyclase by heat-labile *Escherichia coli* enterotoxin. Evidence for ADP-ribosyltransferase activity similar to that of choleragen. J. Clin. Invest. **62:**281–285.
28. **Nikaido, H.** 2003. Molecular basis of bacterial outer membrane permeability revisited. Microbiol. Mol. Biol. Rev. **67:**593–656.
29. **Qadri, F., A. Saha, T. Ahmed, A. A. Tarique, Y. A. Begum, and A.-M. Svennerholm.** 2007. Disease burden due to enterotoxigenic *Escherichia coli* in the first 2 years of life in an urban community in Bangladesh. Infect. Immun. **75:**3961–3968.
30. **Raetz, C. R.** 1993. Bacterial endotoxins: extraordinary lipids that activate eucaryotic signal transduction. J. Bacteriol. **175:**5745–5753.
31. **Russel, M.** 1998. Macromolecular assembly and secretion across the bacterial cell envelope: type II protein secretion systems. J. Mol. Biol. **279:**485–499.
32. **Sambrook, J., E. F. Fritsch, and T. Maniatis.** 1989. Molecular cloning: a laboratory manual. Cold Spring Harbor Press, Cold Spring Harbor, NY.
33. **Sixma, T. K., S. E. Pronk, K. H. Kalk, E. S. Wartna, B. A. van Zanten, B. Witholt, and W. G. Hol.** 1991. Crystal structure of a cholera toxin-related heat-labile enterotoxin from *E. coli*. Nature **351:**371–377.
34. **Sjöling, A., F. Qadri, M. Nicklasson, Y. A. Begum, G. Wiklund, and A. M. Svennerholm.** 2006. In vivo expression of the heat stable (*estA*) and heat labile (*eltB*) toxin genes of enterotoxigenic *Escherichia coli* (ETEC). Microbes Infect. **8:**2797–2802.
35. **Spangler, B. D.** 1992. Structure and function of cholera toxin and the related *Escherichia coli* heat-labile enterotoxin. Microbiol. Rev. **56:**622–647.
36. **Tauschek, M., R. J. Gorrell, R. A. Strugnell, and R. M. Robins-Browne.** 2002. Identification of a protein secretory pathway for the secretion of heat-labile enterotoxin by an enterotoxigenic strain of *Escherichia coli*. Proc. Natl. Acad. Sci. USA **99:**7066–7071.
37. **Tsuji, T., T. Honda, T. Miwatani, S. Wakabayashi, and H. Matsubara.** 1985. Analysis of receptor-binding site in *Escherichia coli* enterotoxin. J. Biol. Chem. **260:**8552–8558.
38. **Turner, S. M., A. Scott-Tucker, L. M. Cooper, and I. R. Henderson.** 2006. Weapons of mass destruction: virulence factors of the global killer enterotoxigenic *Escherichia coli*. FEMS Microbiol. Lett. **263:**10–20.
39. **Vicente, A. C. P., L. F. M. Teixeira, L. Iniguez-Rojas, M. G. Luna, L. Silva, J. R. C. Andrade, and B. E. C. Guth.** 2005. Outbreaks of cholera-like diarrhoea caused by enterotoxigenic *Escherichia coli* in the Brazilian Amazon rainforest. Trans. R. Soc. Trop. Med. Hyg. **99:**669–674.
40. **Wai, S. N., A. Takade, and K. Amako.** 1995. The release of outer membrane vesicles from the strains of enterotoxigenic *Escherichia coli*. Microbiol. Immunol. **39:**451–456.
41. **Wülfing, C., and R. Rappuoli.** 1997. Efficient production of heat-labile enterotoxin mutant proteins by overexpression of *dsbA* in a *degP*-deficient *Escherichia coli* strain. Arch. Microbiol. **167:**280–283.
42. **Yethon, J. A., E. Vinogradov, M. B. Perry, and C. Whitfield.** 2000. Mutation of the lipopolysaccharide core glycosyltransferase encoded by *waaG* destabilizes the outer membrane of *Escherichia coli* by interfering with core phosphorylation. J. Bacteriol. **182:**5620–5623.